# A SEARCH FOR NUCLEAR REACTIONS IN DEUTERATED FRESH IODIDE-TITANIUM FILMS

NUCLEAR REACTIONS IN SOLIDS

**KEYWORDS:** *deuterated titanium films, neutron production, D-D reactions*

FERMÍN CUEVAS, JOSÉ FRANCISCO FERNÁNDEZ, and CARLOS SÁNCHEZ*
*Universidad Autónoma de Madrid, Departamento de Física de Materiales C-IV Facultad de Ciencias, Cantoblanco, 28049 Madrid, Spain*

Received November 22, 1996
Accepted for Publication April 4, 1997

*The possible occurrence of nuclear reactions in solids (NRS) is tested in a well-characterized iodide-titanium film after a high deuterium loading. This film proves to have a higher purity than common titanium samples used in NRS experiments. The titanium deuteration is accomplished in the same chamber where the film is grown to avoid any superficial contamination of the sample. A complete set of NRS experiments is performed, checking as triggering mechanisms of the NRS phenomena the imposition of different electric fields and the crossing of the $\delta$-$\epsilon$ and $\beta$-$\delta$ boundary phases of the Ti-D system. Neutron measurements are monitored while doing these experiments, and no clear evidence of the nuclear fusion reaction $D + D \rightarrow {}^3He + n$ is detected; the detection limit for this reaction is $\Lambda = 3 \times 10^{-21}$ fusions per pair of deuterons per second. However, some anomalous neutron signals are monitored by one of the detectors, which makes further investigation desirable.*

## INTRODUCTION

Since the announcement in 1989 of the detection of the phenomenon of nuclear reactions in solids (NRS) near room temperature,[1-3] a great number of experiments have been performed to establish the conditions necessary to promote these reactions. Until now, both positive and negative results have been published on the existence of NRS; however, unfortunately, the positive results are not completely reliable because of their characteristic irreproducibility. Nevertheless, our present knowledge of NRS indicates that at least some conditions are necessary, in general, to achieve these phenomena:

1. a high deuterium loading of the solid metal matrix[4-6]
2. the imposition of nonequilibrium perturbations in the deuterated metal[7-9]
3. the use of a metal matrix with suitable physical and chemical properties.[10,11]

Much effort has been put forth in the past concerning the first two conditions, but little attention has been paid to the properties that the initial metal must fulfill to be used successfully in NRS experiments. If as a first step one considers that the achievement of room temperature fusion reactions is made possible by the presence of a crystalline environment, one must accept that the physical and chemical characteristics of the metal matrix have to play an essential role in the process. From this point of view, the lack of reproducibility that has been found in many experimental results could be associated with deficient control of the metal matrix properties. In fact, there are some publications[11-15] that reflect on the crucial influence of the properties of the metal on the achievement of NRS. Several authors claim to have detected the phenomenon only in some deuterated palladium samples produced in a certain commercial batch[12] and even from a unique commercial plate.[13] Other authors assert that NRS was detected only in metals with a high concentration of dislocations[11,14] or with a high density of vacancies.[15]

Taking the foregoing considerations into account, we have incorporated in our laboratory an extensive program to produce suitable samples for NRS experiments. To achieve this goal, we have followed in the previous years a detailed investigation to obtain titanium samples by a technique based on the iodide process.[16] This technique provides highly pure titanium metal, called iodide-

*E-mail: sanchez@ccuam3.sdi.uam.es.

titanium, because of the very low reactivity of iodine with titanium oxides, nitrides, and carbides. It is well known that the presence of gaseous interstitial impurities in titanium reduces its maximum deuterium uptake because such impurities also occupy similar sites in the metal matrix. Therefore, a high deuterium loading of the metal can be performed in iodide-titanium samples, as required by the first of the aforementioned conditions.

The experimental procedure designed in this research for the deposition of titanium films allows one to accomplish gas deuterium loading of the sample without any surface-blocking effects, as the deposited film is never exposed to air. In addition, the titanium film is deposited over a self-heated tungsten filament that is held by thick electrodes. This configuration permits one to pass high electric currents through the film, after its deuteration, which are used for the variation of the film temperature and the imposition of nonequilibrium disturbances in it, as required by the second condition, by means of different electric field patterns. The possible existence of nuclear reactions under these circumstances is checked by neutron measurements, as the detection of such particles would indicate without doubt the nuclear nature of the NRS phenomenon.

## EXPERIMENTAL

### Characteristics of the Sample

Many iodide-titanium samples were produced in our laboratory with different deposition parameters to obtain suitable samples for NRS experiments.[17,18] The iodide technique was accomplished by the flow of $TiI_4$ vapors through an electrically heated tungsten filament with typical dimensions of $40 \times 2 \times 0.025$ mm$^3$. Titanium films were deposited uniformly over these tungsten substrates up to a typical mass of 55 mg. Among the main deposition parameters, the $TiI_4$ vapor pressure and the substrate temperature, it was found that the latter parameter is the most important to achieve pure titanium films because it dictates the observed substrate diffusion into the film. As we pointed out in Ref. 19, the presence of tungsten in titanium reduces its maximum hydrogen uptake, so that low substrate temperatures are required during deposition. The substrate temperature range that favors the titanium deposition by the iodide process was established in our study to be 1450 to 1800 K.

All the NRS experiments presented in this paper were accomplished with a unique iodide-titanium sample. This sample was never exposed to the open air to avoid any superficial oxidation that would interfere with the deuterium absorption into the sample and its loading capacity. Therefore, a twin titanium film was deposited with the same growth parameters, at a low substrate temperature (1485 K), to conduct a proper characterization. The composition and crystalline state of the twin sample were analyzed by scanning electron microscopy, energy dispersive X rays (EDX), Auger electron spectroscopy (AES), and X-ray diffraction (XRD).

The backscattered electron (BSE) image of the twin-sample cross section is shown in Fig. 1. Three different layers can be observed in the sample: the tungsten substrate in the middle (the white layer), followed by deposited titanium where some diffused tungsten is present (the bright gray layer), and finally the pure titanium film in the outer part of the sample (the dark gray layer). The performed EDX analysis revealed a maximum tungsten content in the diffused layer of 9 at.%, while no metallic impurities were detected in the pure titanium film at a typical detection sensitivity of 0.2 at.%. In relation to the presence of gaseous impurities, the AES spectrum of the twin sample at a depth of 200 Å is shown in Fig. 2. The energy position of very low signals due to the presence of gaseous impurities (carbon, nitrogen, and oxygen) is indicated by arrows. A quantitative analysis of the spectrum yields the following concentrations: carbon $< 1.5$ at.%, nitrogen $< 2$ at.%, and oxygen $= 2$ at.%. To compare this analysis with the presence of impurities in commercial samples, which are currently used in NRS experiments, another AES spectrum was collected from a commercial titanium sample of 99.6% nominal purity, and it showed a gaseous impurity content ten times higher than that of our iodide-titanium film. Therefore, one may conclude that in principle, the selected sample is more suitable for NRS experiments than is typical commercial samples.

The crystalline state of the twin sample was studied by XRD and microscopy observations. The XRD pattern

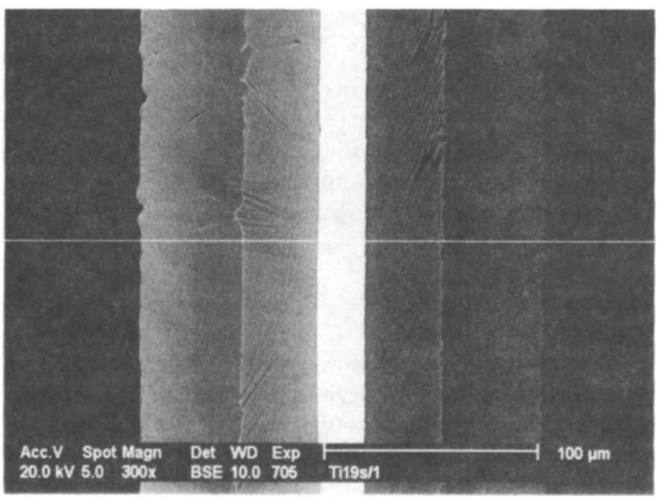


Fig. 1. BSE image of the twin-sample cross section identical to the one used in the NRS experiments. The tungsten substrate appears as a white band in the middle of the film. The following layers can be discerned in the deposited titanium: a bright gray layer where some diffused tungsten is present and a dark gray layer corresponding to pure titanium.

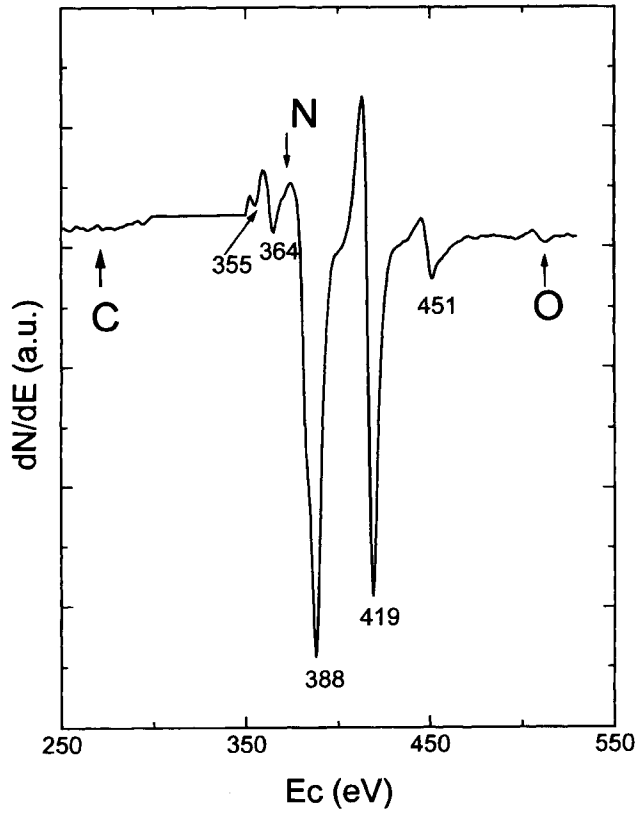


Fig. 2. AES spectra of the twin sample at 200-Å depth. The energy positions of gaseous impurities are depicted by arrows. The kinetic energy values of the titanium electronic transitions are indicated.

revealed that most of the crystallographic planes of the $\alpha$-titanium metal are present on the film surface, which is formed by equiaxed grains of $\cong 1$ $\mu$m in diameter. This structure corresponds to that of typical well-annealed samples. However, the crystallite size of the film was found to be ~60 nm, so that an appreciable number of dislocations exist in every crystalline titanium grain.

### Experimental Setup for the NRS Experiments

The complete arrangement of the experimental system used in the NRS experiments is shown in Fig. 3. It essentially consists of two different types of equipment: One deals with the thermodynamical and electrical control of the iodide-titanium film (upper part of Fig. 3), and the other deals with the neutron detection system (lower part of Fig. 3). Both parts, which are time interconnected, are described as follows.

The iodide-titanium sample, which is supported by two tungsten electrodes, is located in the middle of the growth reaction chamber. These electrodes allow one to pass an electric current, which is generated by a direct-current (dc) power supply[a] controlled by a function synthesizer,[b] through the film. In addition, two thin tungsten wires are welded to the edges of the sample, so that the well-known four-probe method is accomplished for resistance measurements. A thermocouple (NiCr-NiAl) is located in the outer part of the reaction chamber to obtain some knowledge of gas temperature in the environment of the sample and for safety precautions. The reaction chamber, initially under vacuum conditions, is made of glass and is connected through a very thin glass separator to a deuteration reservoir. The whole set constitutes a Sieverts-type apparatus composed of two volumes: the reservoir chamber ($V = 77.5 \pm 1.5$ ml) and the reaction chamber ($V = 374 \pm 10$ ml). The reservoir chamber is attached to a deuterium inlet (purity 99.999%) and also to a turbomolecular pump and is equipped with a piezoresistive transducer[c] and a penning gauge. All thermodynamic and electrical parameters are monitored by a personal computer with an acquisition time of 10 s.

The neutron detection measurements were carried out by two liquid scintillation counters (NE-213[d] and BC-501[e]). The $\gamma$-$n$ discrimination of the scintillation counters was accomplished by two electronic systems using a pulse-shape-discrimination technique. Both energy spectra and counting time evolution were finally recorded in different multichannel analyzers (MCAs). In the case of the counting time evolution, the detected neutrons (namely, counts) were collected every 20 s, while in the energy spectra the counts were integrated during the duration time of every experiment (typically 9 h). The absolute efficiency of the detectors, taking also into account the geometrical configuration of the setup, were $6.6 \times 10^{-4}$ for NE-213 and $5.7 \times 10^{-3}$ for BC-501 at the interesting energy of 2.45 MeV, corresponding to the D + D $\rightarrow$ $^3$He + $n$ reaction. The background counting rates of the detection systems were $5.3 \times 10^{-3}$ and 0.26 count/s, respectively. Further information about calibration of the equipment and other technical characteristics can be found elsewhere.[20,21]

### Sample Deuteration and NRS Experimental Procedures

To perform the deuteration of the titanium film, one must first evacuate the reservoir chamber down to $10^{-5}$ Torr, and then deuterium gas is admitted into this chamber. As was mentioned earlier, the reaction chamber is kept in vacuum after titanium deposition, and it is now when both chambers are connected by crashing the glass separator with a magnetic striker. Afterward, the deuterium pressure is fixed to 300 mbar, and connections

[a]The dc power supply is a Kenwood PD35-20D.
[b]The function synthesizer is a Keithley 3910.
[c]The piezoresistive transducer is a Kistler 4043A.
[d]The NE-213 scintillator is from Nuclear Enterprise.
[e]The BC-501 scintillator is from Bicron Corporation.

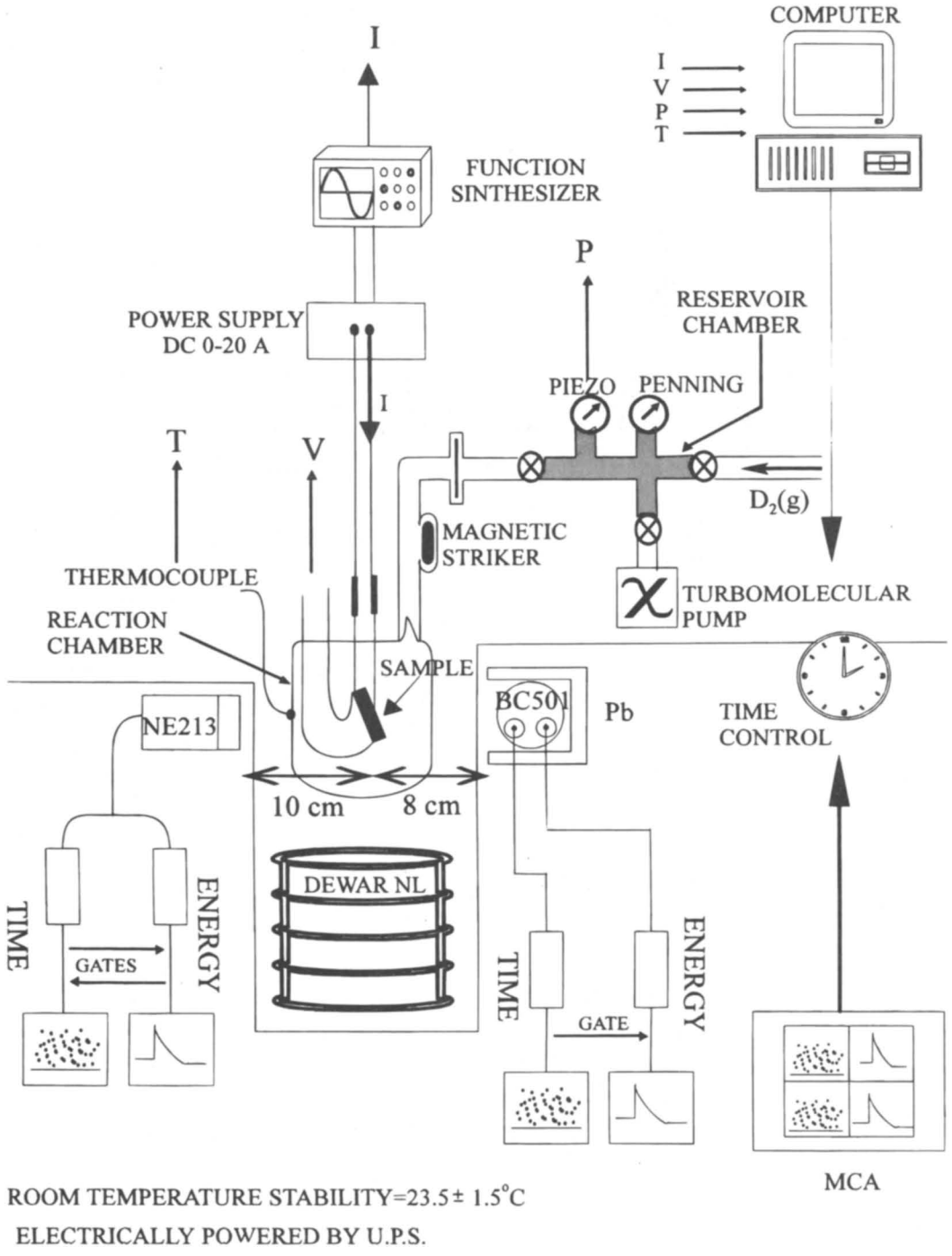


Fig. 3. Sketch of the experimental system used for the sample deuteration and the performance of NRS experiments.

to vacuum and deuterium inlets are closed so that both chambers form a closed system. Under these circumstances, the sample is heated to a glowing temperature (1200 K) by passing a high dc (13 A) through it. Finally, a decreasing electric ramp is programmed through the sample to cool it down slowly to room temperature, leading to the deuterium absorption into the film as dictated by the characteristics of the P-X-T phase diagram[22] of Ti-D. The average deuterium concentration in the titanium film after this treatment was evaluated, from the overall pressure drop in the system, to be $TiD_{1.5\pm0.3}$. As the presence of tungsten in titanium reduces the deuterium absorption in the diffused layer, a higher deuterium content is expected in the pure titanium layer, which,

therefore, should at least be in the high concentrated $\delta$-phase ($x \geq 1.6$).

Once a high deuterium concentration is achieved in the sample, it is necessary to provoke nonequilibrium conditions in the system to trigger the NRS phenomenon. To this aim, we performed two different sets of experiments. In the first set, we applied different electric fields in the sample by passing different electric current patterns through it. The second set of experiments deals with the possible influence of phase transitions on the achievement of NRS.

The imposition of electric fields in a solid deuteride system induces important perturbations in the system such as electromigration processes[23] and the presence of ampere forces.[24] From an empirical point of view, note that electronic fields are also present in the electrochemical NRS experiments, where many positive results of the production of room temperature fusion reactions have been claimed. Considering these possibilities, three experiments were performed, denoted Exp 1, Exp 2, and Exp 3, that corresponded to different electric current patterns, as shown in Fig. 4. In Exp 1, two constant electric currents of $\cong$1 and $\cong$4 A were passed through the sample. In Exp 2, the electric current was changed abruptly between 0.2 and 3 A at a frequency of 0.8 mHz. Finally, in Exp 3, a triangular current pattern between 0 to 7 A at a frequency of 0.4 mHz was programmed. While all these experiments were done, the neutron counts were recorded simultaneously, as shown in Fig. 5 for Exp 1.

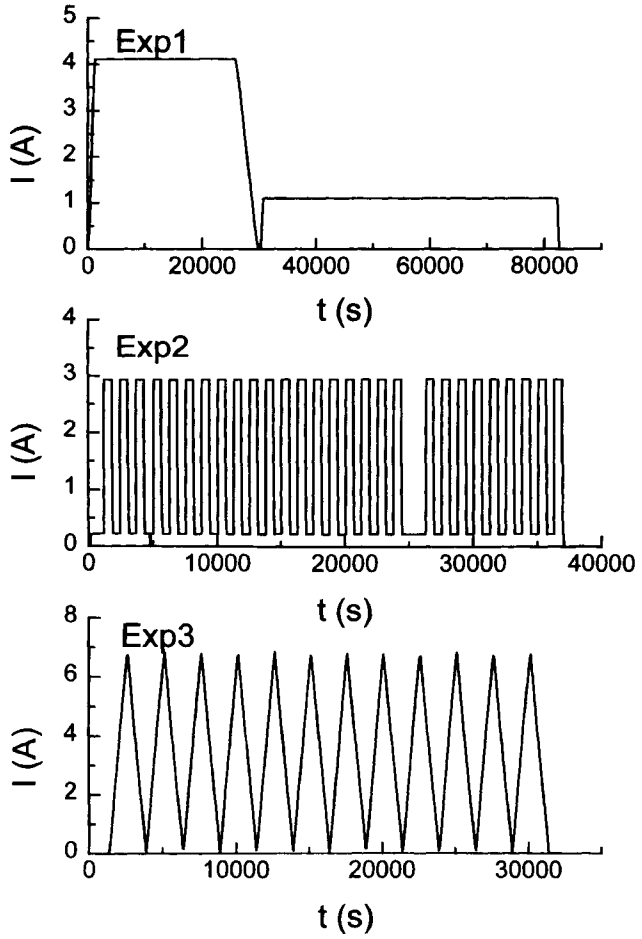


Fig. 4. Time evolution of the electric current patterns imposed on the sample in Exps 1, 2, and 3.

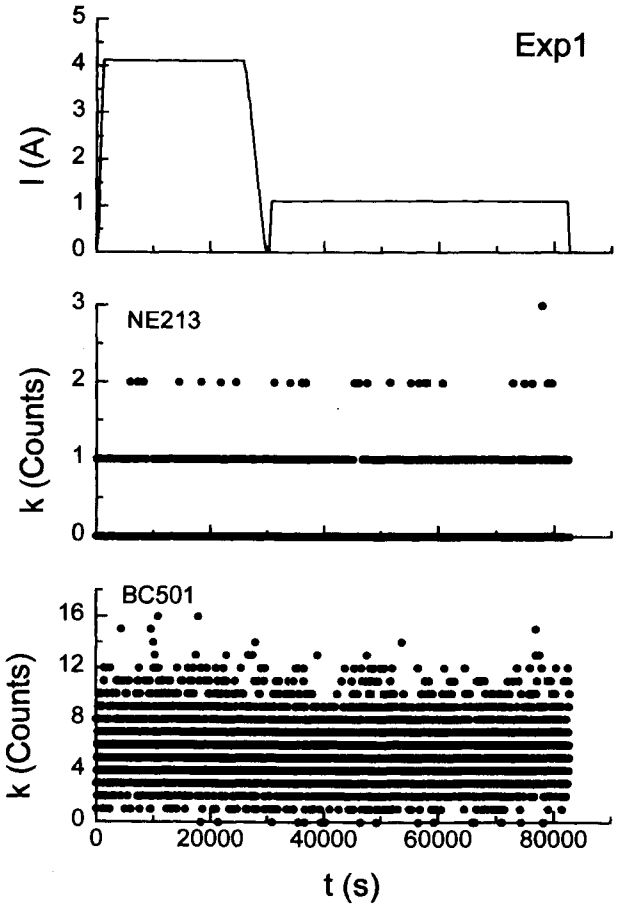


Fig. 5. Time evolution of the electric current and detected neutrons at $t_i$ = 20 s in Exp 1.

In relation to phase transition experiments, some research reports the occurrence of NRS in titanium deuteride when this system is thermally cycled at about room temperature,[3,25–27] which can be related to the $\delta$-$\epsilon$ phase transition, or at about the $\beta$-$\delta$ phase transition itself.[25–28] To check these triggering conditions, we performed two experiments, Exps 4 and 5, in which the sample was forced to undergo the aforementioned transitions. To provoke the $\delta$-$\epsilon$ phase transition (Exp 4), the reaction chamber was immersed in a liquid nitrogen dewar; meanwhile, triangular electric current cycles up to 9.5 A were passed through the sample. This procedure induced thermal cycling of the sample from a nearly liquid nitrogen temperature to some value above room temperature, as was

checked from sample resistivity measurements. Twelve of these cycles were programmed at a frequency of 0.4 mHz. In Fig. 6a, the evolution of the sample resistance, and its derivative, during the ascending part of the third electric current cycle is presented. Note that the sample resistance exceeds its room temperature value (which was measured before the experiment). Gesi et al.[30] report that the resistivity of the titanium deuteride suffers a slight discontinuity during the $\delta$-$\epsilon$ transition. However, we were unable to observe clearly such behavior, although some fluctuations were observed near room temperature in the *dR/dI* derivative function. This result would imply that perhaps we were able to produce the transition only in some parts of the sample. Finally, the $\beta$-$\delta$ transition was provoked in Exp 5 by cycling a high-current electric pattern between 6 and 13 A through the sample with an initial deuterium pressure of 300 mbar in the closed reactor. Sixteen triangular-shaped cycles were conducted at a frequency of 0.8 mHz and 16 more at a double speed. To verify the accomplishment of this transition we simultaneously monitored both the electric resistance of the sample and the deuterium pressure in the closed reactor. Note in Fig. 6b the relationship between both parameters in one of the cycles, which without doubt reflects the mentioned transition, as has been discussed elsewhere.[29]

### Neutron Count Analysis

To examine the possible existence of the NRS phenomenon in the described experiments, it is indispensable to compare the neutron measurements that are monitored during the experiments with those corresponding to the natural background. To this end, we recorded the background signals for 11 days after completing the NRS experiments. It is well known that the neutron time counting is more sensitive to detecting the possible neutron emissions from the sample than the characteristics of the energy spectra. Therefore, it is more convenient to analyze the neutron time evolution during the experiments and afterward, if significant signals are detected in comparison with the background level, to look for the energy value of the detected neutrons. On the other hand, as the time pattern of the emitted neutrons is unknown in advance (e.g., bursts or time-continuous emissions), it is necessary to analyze the neutron counting rate for different integration times. Selected integration times ($t_i$) for these analyses are 20 s, corresponding to the minimum acquisition time in the experiments; 1200 s, corresponding to the typical time of electric current cycling frequency, and 9 h, corresponding to the typical elapsed time of the experiments.

The frequency distribution of neutron counts must obey a Poisson distribution if they originated from random phenomena, as is essentially expected for the natural background. This behavior is shown in Fig. 7a, where the absolute frequency distribution of the natural background at $t_i$ = 20 s for the BC-501 is compared to the Poisson distribution that corresponds to the average value of the neutron counts ($\lambda$) during $t_i$. To discern neutron emissions during the experiments from the Poisson background, one should establish a confidence level that dictates the neutron detection limit of the system. Taking 99.9% as the confidence level, the detection limit for BC-501 is 15 counts at $t_i$ = 20 s, corresponding to a neutron emission rate of 85 n/s. This detection limit implies that if 15 or more counts/20 s are detected by the BC-501

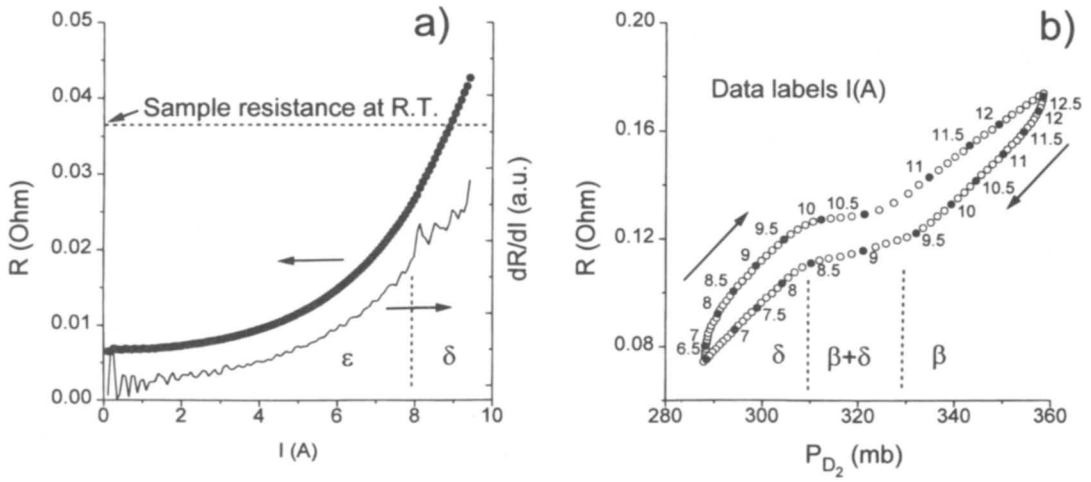


Fig. 6. Observation of the (a) $\delta$-$\epsilon$ and (b) $\beta$-$\delta$ phase transitions in Exps 4 and 5, respectively. In (a), the evolution of the sample electric resistance (black dots) and its derivative (continuous line) compared with the electric current, during the ascending part of the third electric current cycle, is given. The value of the sample electric resistance at room temperature is also depicted. In (b), the relationship between sample electric resistance and deuterium pressure in the closed reactor, during the entire electric current cycle, is shown.[29]

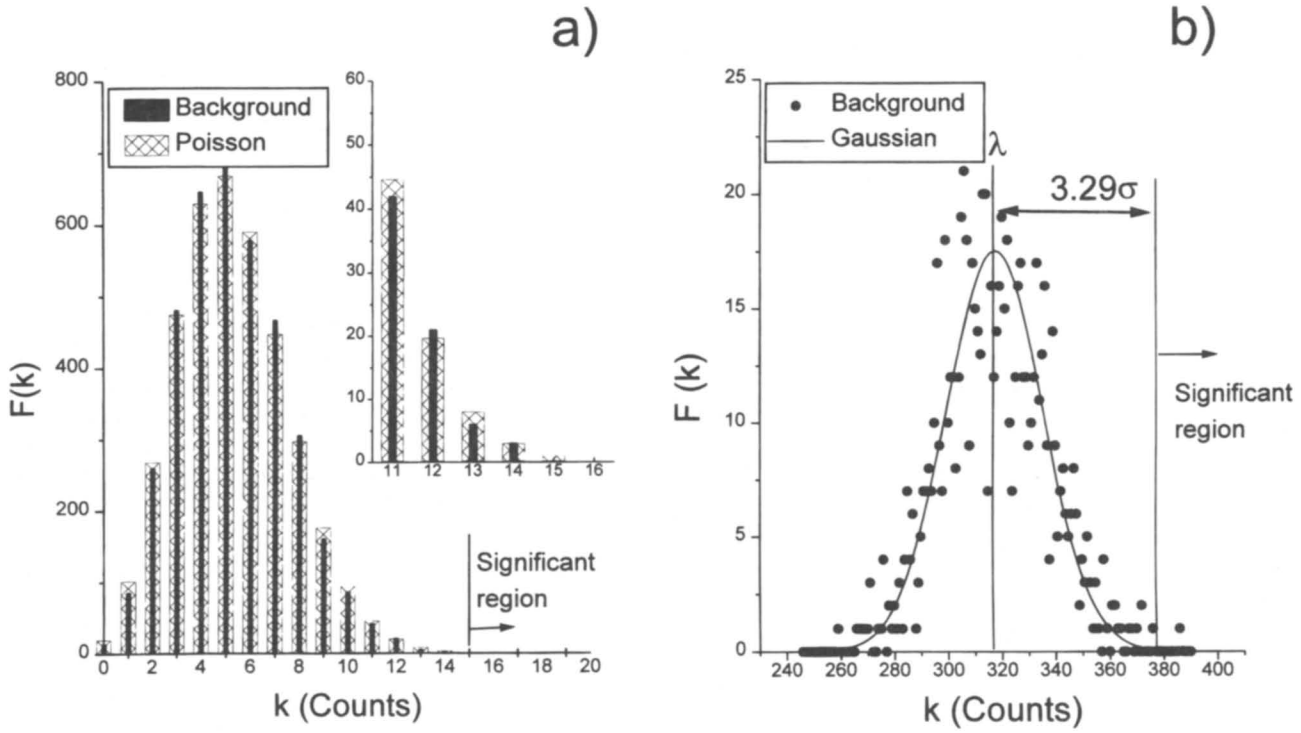


Fig. 7. Absolute frequency of the neutron background detected by the BC-501 system at integration times of (a) 20 s and (b) 1200 s. In (a), the detected counts are depicted by black bars, and the Poisson distribution corresponding to the average value of the detected counts is represented by pattern bars. The significant region corresponding to a confidence level of 99.9% is expressly pointed out. In (b), the detected counts are depicted by black dots, and the Gaussian distribution corresponding to the average value of the detected counts is represented by a continuous line. The significant region corresponding to a confidence level of 99.9% is expressly pointed out.

system, they can be considered as NRS significant signals with a confidence of 99.9%.

A similar analysis has been performed for the other $t_i$ values. At $t_i = 1200$ s, the Poisson distribution approaches Gaussian, as the value of $\lambda$ considerably increases (Fig. 7b). The confidence level of 99.9% corresponds now to a deviation value of 3.29 $\sigma$ from $\lambda$, the detection limit in the BC-501 is 377 counts/1200 s, and the neutron emission rate is 9 n/s. Finally, at $t_i = 9$ h, the registered background time is insufficient to obtain good approximations to a statistical function. Nevertheless, note that we are still dealing with a Gaussian distribution and may take the deviation value of the neutron counting for significant signals as $3.29\sigma$. However, the Tchebychev theorem states that the confidence level for this assumption is only 90%. The minimum neutron emission that can be detected in the BC-501 is in this case 3 n/s. This detection limit implies, considering the sample titanium mass (55 mg) and its deuterium content ($X = 1.5$), a neutron detection rate limit of $\Lambda = 3 \times 10^{-21}$ fusions per pair of deuterons per second (f/pds). In Table I, the neutron detection limits for both detection systems at the different integration times are summarized.

## RESULTS AND DISCUSSION

The neutron measurements monitored while doing all the described NRS experiments were analyzed for every integration time and compared with the neutron

TABLE I

Neutron Detection Limits in the NE-213 and BC-501 Systems at Different Integration Times $t_i$*

| | NE-213 | | BC-501 | |
|---|---|---|---|---|
| $t_i$ | Neutron Detection Limit (n/s) | Significant Counting Level (count) | Neutron Detection Limit (n/s) | Significant Counting Level (count) |
| 20 s | 220 | 3 | 85 | 15 |
| 1200 s | 11 | 15 | 9 | 377 |
| 9 h | 2 | $\lambda + 3.29\sigma$ | 3 | $\lambda + 3.29\sigma$ |

*The detection limit is given as neutrons per second emitted from the sample and counts per $t_i$ detected by the equipment.

background. Note that the electronic system associated with the NE-213 detector suffered a misfunction during Exp 4, so that no neutron data will be offered for this detector in Exp 4. All other neutron data are now presented and discussed.

The highest values of counting rate registered at $t_i$ = 20 s for every experiment are summarized in Table II. For this value of $t_i$, the significant events respond to a counting rate equal to or higher than 3 counts in NE-213 and 15 in BC-501. The most anomalous result was found in Exp 1, in which 3 counts were detected once in NE-213 and 16 counts were detected twice in BC-501. Nevertheless, the absolute frequency of these events for the background Poisson distribution is still important: 0.76 for NE-213 and 0.37 for BC-501. Such nonnegligible values account for the large number of registered intervals, that is, more than four thousand. In addition, there is no time correlation between the significant signals in both detectors. Therefore, in spite of the detection of these anomalous events, we cannot assert the presence of the NRS phenomenon at short integration times ($t_i$ = 20 s) with a detection limit of $\approx$100 n/s.

The most significant signals of neutron detection at $t_i$ = 1200 s, corresponding to the typical cycling time, are presented in Table III. At this integration time, the significant events are those with counting rates equal to or higher than 15 counts in NE-213 and 377 counts in BC-501. While no significant events have been detected in NE-213, some significant ones were observed in BC-501. The most outstanding events present a deviation from the background average of $5.0\sigma$ (Exp 3) and $4.3\sigma$ (Exp 5). Note that both experiments were done with similar electric current patterns: triangular-shaped waves reaching high electric current values. The neutron counting in BC-501 and the electric current time evolution for both experiments are shown in Fig. 8. Observe that the

TABLE II

Significant Events Monitored by the Neutron Detection Systems at $t_i$ = 20 s*

| | Exp 1 | Exp 2 | Exp 3 | Exp 4 | Exp 5 |
|---|---|---|---|---|---|
| NE-213 | | | | | |
| $k$-$F(k)$ | 3(1) | 2 | 3(1) | | 2 |
| $F(k)$ background | 0.76 | | 0.29 | | |
| BC-501 | | | | | |
| $k$-$F(k)$ | 16(2) | 15(1) | 16(1) | 16(1) | 14 |
| $F(k)$ background | 0.37 | 0.51 | 0.14 | 0.15 | |

*The $k$-$F(k)$ indicates the highest counting value in the experiments and its absolute frequency (in parentheses). The $F(k)$ background stands for the absolute frequency in the Poisson background of the monitored significant events during the experiments. The absolute frequency is given only for significant events.

TABLE III

Significant Events Monitored by the Neutron Detection Systems at $t_i$ = 1200 s*

| | Exp 1 | Exp 2 | Exp 3 | Exp 4 | Exp 5 |
|---|---|---|---|---|---|
| NE-213 | | | | | |
| $k$-$F(k)$ | 13 | 12 | 13 | | 13 |
| $\Delta k$ | | | | | |
| BC-501 | | | | | |
| $k$-$F(k)$ | 380(2) | 375 | 407(1) | 366 | 395(1) |
| $\Delta k$ | $3.5\sigma$ | | $5.0\sigma$ | | $4.3\sigma$ |

*The $k$-$F(k)$ indicates the highest counting value in the experiments and its absolute frequency (in parentheses). The $\Delta k$ stands for the deviation of the monitored significant events from the average background value. The absolute frequency is given only for significant events.

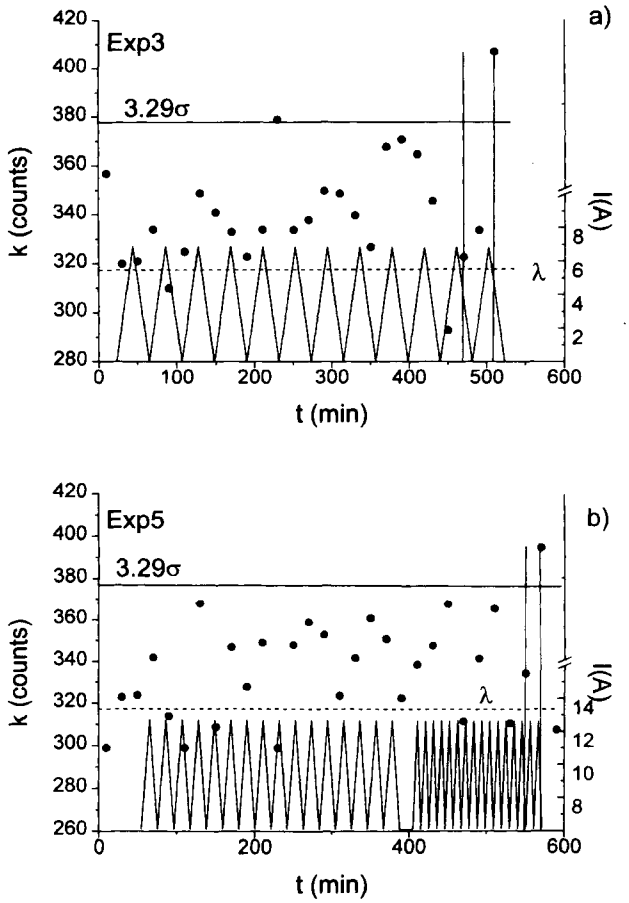


Fig. 8. Counting time evolution detected by the BC-501 system at $t_i$ = 1200 s in Exps 3 and 5. The electric current time evolution in these experiments is also depicted. The horizontal dotted lines indicate the average counting value of the background ($\lambda$). The horizontal continuous lines stand for a deviation value of $+3.29\sigma$ from $\lambda$. The different counting rate between two events monitored at identical electrodynamical conditions is indicated by vertical continuous lines.

significant events were detected in both cases after the imposition of many electric current cycles and also that the detected counts in every interval often have a higher value than the background average level. All these observations could indicate a slight neutron emission from the titanium deuteride film; however, other facts contradict this possibility. First, as was previously pointed out, no significant events were detected by NE-213, being that the detection limit for both scintillation counters was practically the same: 11 n/s in NE-213 and 9 n/s in BC-501. Second, no correlation was found in every experiment itself between the significant events and similar electrodynamic states, as is denoted in Fig. 8 by the vertical lines. In other words, while imposing the same electrical conditions on the sample, significant events were not always detected. From this point of view, the significant events detected by BC-501 could possibly be related to a shift in the natural background or to a small drift in the electronic system associated with this detector. In conclusion, it is not possible to claim for sure the presence of the NRS phenomenon in the conducted experiments with a time pattern similar to the electric current cycling frequencies. Nevertheless, future experiments that would check if long electric cycling at high currents could induce the presence of the NRS phenomenon in titanium deuteride would be desirable.

Finally, the entire neutron counting for every experiment was analyzed, and the results are presented in Table IV and Fig. 9. The results match well with the background measurements, except in the case of the detected counts by BC-501 in Exp 3, where a deviation of $3.6\sigma$ from the background average was monitored. In any case, this possible neutron emission was not corroborated by NE-213. Note also that the collected counts in most of the cases are higher than the background average recorded after completion of the NRS experiments, indicating a possible shift of the registered background level. To conclude, there was no detection of any continuous NRS phenomenon in these experiments at a detection limit of 2 n/s, corresponding to a fusion nuclear reaction rate in the sample of $\Lambda = 3 \times 10^{-21}$ f/pds. Note also that we cannot confirm a deuteration of the titanium film higher than $x = 1.6$. Therefore, it is possible that the lack of presence of nuclear reactions could be related to an insufficient loading of the sample if a minimum loading ratio of $x = 1.95$ is needed, as we suggested previously in Ref. 6.

## CONCLUSIONS

A complete set of NRS experiments were performed after deuteration of a high pure iodide-titanium film. The physical and chemical characteristics of the initial metal were deeply analyzed in relation to the content of interstitial gaseous impurities (carbon $< 1.5$ at.%, nitrogen $<$ 2 at.%, and oxygen = 2 at.%) and crystallographic properties. A titanium film grown in our laboratory was subjected to different electric fields and was forced to undergo the $\delta$-$\epsilon$ and $\beta$-$\delta$ phase transitions to trigger deuterium fusion reactions in the Ti-D system. Neutron measurements monitored during these experiments were analyzed considering distinct time patterns and were compared with the natural background. No clear evidence of the presence

TABLE IV

Total Counts Monitored by the Neutron Detection Systems for the Entire Experimental Time*

| | Exp 1 | Exp 2 | Exp 3 | Exp 4 | Exp 5 |
|---|---|---|---|---|---|
| | Experiment Time(s) | | | | |
| | 82 680 | 37 200 | 31 680 | 34 080 | 36 360 |
| NE-213 | | | | | |
| Total counts | 439 | 222 | 176 | — | 222 |
| $\lambda$ background | 441 | 198 | 169 | 182 | 193 |
| ($\lambda + 3.29\sigma$) background | 523 | 244 | 205 | 225 | 239 |
| BC-501 | | | | | |
| Total counts | 22 693 | 10 422 | 9005 ($3.6\sigma$) | 9337 | 10 146 |
| $\lambda$ background | 21 842 | 9 841 | 8381 | 9017 | 9 588 |
| ($\lambda + 3.29\sigma$) background | 22 977 | 10 459 | 8953 | 9589 | 10 160 |

*The $\lambda$ background stands for the average background counts during the experimental time and the ($\lambda + 3.29\sigma$) background corresponds to the number of counts at a deviation of $3.29\sigma$ from the $\lambda$ background. The deviation of significant events is given in parentheses.

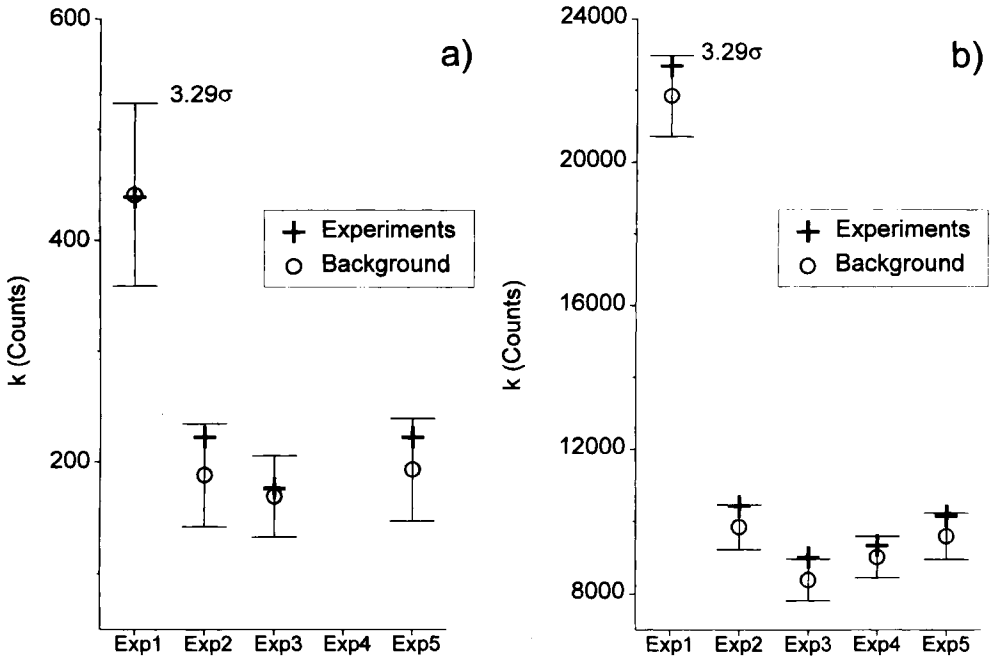


Fig. 9. Neutrons detected by the (a) NE-213 system and (b) BC-501 system during the entire elapsed time of every experiment. The experimental data are represented by cross symbols, the background signal average ($\lambda$) by circular symbols, and the deviation of $\pm 3.29\sigma$ from $\lambda$ by error bars.

of the NRS phenomenon during experiments was found; the detection limit for the rate of the D + D $\rightarrow$ $^3$He + $n$ reaction was $\Lambda = 3 \times 10^{-21}$ f/pds. Nevertheless, some anomalous events were monitored in one of the neutron detectors when multiple electric current cycles up to high values were performed in the sample, which suggests further investigation.

## ACKNOWLEDGMENTS

Financial support from the Spanish Direccion General de Investigacion Cientifica y Tecnica is gratefully acknowledged (PB93-0266). Technical assistance from F. Moreno, A. Bergas, and Servicios generales de apoyo a la investigacion experimental is also recognized. Special thanks are given to J. A. Rubio (CERN) for providing the $D_2$ gas and M. Fernández (Instituto Torres Quevedo, Consejo Superior de Investigaciones Cientificas) for the Auger electron spectroscopy measurements.

## REFERENCES

1. M. FLEISCHMANN and S. PONS, "Electrochemical Induced Nuclear Fusion of Deuterium," *J. Electroanal. Chem.*, **261**, 301 (1989).

2. S. E. JONES et al., "Observation of Cold Nuclear Fusion in Condensed Matter," *Nature*, **338**, 737 (1989).

3. A. DE NINNO et al., "Evidence of Neutron Emission from a Titanium-Deuterium System," *Europhys. Lett.*, **9**, *3*, 221 (1989).

4. M. C. H. McKUBRE, S. CROUCH-BAKER, A. M. RILEY, S. I. SMEDLEY, and F. L. TANZELLA, "Excess Power Observations in Electrochemical Studies of the D/Pd System: The Influence of Loading," *Frontiers of Cold Fusion*, p. 5, H. IKEGAMI, Ed., Universal Academy Press, Tokyo (1993).

5. K. KUNIMATSU, H. HASEGAWA, A. KUBOTA, N. IMAI, M. ISHIKAWA, H. AKITA, and Y. TSUCHIDA, "Deuterium Loading Ratio and Excess Heat Generation During Electrolysis of Heavy Water by a Palladium Cathode in a Closed Cell Using a Palladium Immersed Fuel Cell Anode," *Frontiers of Cold Fusion*, p. 31, H. IKEGAMI, Ed., Universal Academy Press, Tokyo (1993).

6. M. ALGUERÓ, J. F. FERNÁNDEZ, F. CUEVAS, and C. SÁNCHEZ, "An Interpretation of Some Postelectrolysis Nuclear Effects in Deuterated Titanium," *Fusion Technol.*, **29**, 390 (1996).

7. A. LEGGET and G. BAYM, "Exact Upper Bond on Barrier Penetration Probabilities in Many Body Systems: Application to Cold Fusion," *Phys. Rev. Lett.*, **63**, 191 (1989).

8. A. LEGGET and G. BAYM, "Can Solid State Effects Enhance the Cold Fusion Rate?" *Nature*, **340**, 45 (1989).

9. V. A. CHECHIN and V. A. TSAREV, "On the Nonstationary Quantum-Mechanical Origin of Nuclear Reactions in Solids," *Fusion Technol.*, **25**, 469 (1994).

10. E. STORMS, "Measurement of Excess Heat from a Pons-Fleischmann Type Electrolytic Cell," *Frontiers of Cold Fusion*, p. 21, H. IKEGAMI, Ed., Universal Academy Press, Tokyo (1993).

11. D. GOZZI et al., "Experiments with Global Detection of Cold Fusion Byproducts," *Frontiers of Cold Fusion*, p. 155, H. IKEGAMI, Ed., Universal Academy Press, Tokyo (1993).

12. H. MIYAMARU and A. TAKAHASHI, "Periodically Current-Controlled Electrolysis of $D_2O$/Pd System for Excess Heat Production," *Frontiers of Cold Fusion*, p. 393, H. IKEGAMI, Ed., Universal Academy Press, Tokyo (1993).

13. X. LI et al., "The Precursor of 'Cold Fusion' Phenomenon in Deuterium/Solid Systems," *Proc. Anomalous Nuclear Effects in Deuterium/Solid Systems*, p. 419, S. E. JONES, F. SCARAMUZZI, and D. H. WORLEDGE, Eds., American Institute of Physics (1991).

14. K. OTA, M. KURATSUKA, K. ANDO, Y. IIDA, H. YOSHITAKE, and N. KAMIYA, "Heat Production of Heavy Water Electrolysis Using Mechanically Treated Pd Cathode," *Frontiers of Cold Fusion*, p. 71, H. IKEGAMI, Ed., Universal Academy Press, Tokyo (1993).

15. F. CELANI, A. SPALLONE, P. TRIPODDI, and A. NUVOLI, "Measurements of Excess Heat and Tritium During Self-Biased Pulsed Electrolysis of Pd-$D_2O$," *Frontiers of Cold Fusion*, p. 93, H. IKEGAMI, Ed., Universal Academy Press, Tokyo (1993).

16. R. F. ROLSTEN, *Iodide Metals and Metal Iodides*, John Wiley & Sons, New York (1961).

17. F. CUEVAS, J. F. FERNÁNDEZ, M. ALGUERÓ, and C. SÁNCHEZ, "On the Necessary Experimental Conditions to Grow Titanium Films on Hot Tungsten Filaments Using Titanium Tetraiodide," *J. Alloys Compounds*, **277**, 167 (1995).

18. F. CUEVAS, "Obtención de Titanio de Alta Pureza por el Proceso de Yoduros y Fenómenos Asociados a su Hidrogenación/Deuteración," Doctoral Thesis, Universidad Autónoma de Madrid (1996) (in Spanish).

19. F. CUEVAS, J. F. FERNÁNDEZ, M. ALGUERÓ, and C. SÁNCHEZ, "The Influence of Tungsten Substrates on Hydrogen Absorption by Iodide Titanium Films," *J. Alloys Compounds*, **231**, 798 (1995).

20. J. F. FERNÁNDEZ, F. CUEVAS, M. ALGUERÓ, and C. SÁNCHEZ, "The Cubic-Tetragonal Phase Transition in $TiD_x$ ($x \geq 1.7$) and Its Possible Relation to Cold Fusion Reactions," *Trans. Fusion Technol.*, **26**, 307 (1994).

21. J. F. FERNÁNDEZ, F. CUEVAS, M. ALGUERÓ, and C. SÁNCHEZ, "Experimental Investigations of Neutron Emissions During Thermal Cycling of $TiD_x$ ($x \approx 2.00$)," *Fusion Technol.*, **31**, 237 (1997).

22. A. SAN MARTIN and F. D. MANCHESTER, "The H-Ti (Hydrogen-Titanium) System," *Bull. Alloy Phase Diagrams*, **8**, 30 (1987).

23. K. G. RAJAN, U. K. MUDALI, R. K. DAYAL, and P. RODRÍGUEZ, "Electromigration Approach to Verify Cold Fusion Effects," *Fusion Technol.*, **20**, 100 (1991).

24. M. RAMBAUT, "Capillary Fusion Through Coulomb Barrier Screening in Turbulent Processes Generated by High Intensity Current Pulses," *Phys. Lett., A*, **163**, 335 (1992).

25. V. F. ZELENSKIJ, V. F. RYBALKO, A. N. MOZOROV, G. D. TOLSTOLUTSKAYA, V. G. KULISH, S. V. PISTYAK, and I. S. MARTYNOV, "Experiments on Cold Nuclear Fusion in Pd and Ti Saturated with Deuterium by Ion Implantation," Preprint KNFTI, TsNIIatominform, Moscow (1989).

26. F. E. CECIL, H. LIV, D. BEDDINGFIELD, and G. S. GALOVICH, "Observation of Charged Particle Bursts from Deuterium Loaded Thin Titanium Foils," *Proc. Anomalous Nuclear Effects in Deuterium/Solid Systems*, p. 375, S. E. JONES, F. SCARAMUZZI, and D. WORLEDGE, Eds., American Institute of Physics (1991).

27. H. O. MENLOVE, M. A. PACIOTLI, T. N. CLAYTOR, H. R. MALTROD, O. M. RIVERA, D. G. TUGGLE, and S. E. JONES, "Reproducible Neutron Emission Measurements from Ti Metal in Pressurized $D_2$ Gas," *Proc. Anomalous Nuclear Effects in Deuterium/Solid Systems*, p. 287, S. E. JONES, F. SCARAMUZZI, and D. WORLEDGE, Eds., American Institute of Physics (1991).

28. I. L. BELTYUKOV et al., "Laser-Induced Cold Nuclear Fusion in Ti-$H_2$-$D_2$-$T_2$ Compositions," *Fusion Technol.*, **20**, 234 (1991).

29. F. CUEVAS, J. F. FERNÁNDEZ, and C. SÁNCHEZ, "Observation of the $\beta$-$\delta$ Phase Transformation in Deuterated Iodide Titanium Films by Electrical Resistance Measurements," *J. Alloys Compounds*, **253–254**, 158 (1997).

30. K. GESI, Y. TAKAGI, and T. TAKEUCHI, "The Hall Effect of Titanium Hydrides," *J. Phys. Soc. Jpn.*, **18**, 306 (1963).

---

**Fermín Cuevas** [MS, physics, Universidad Autonoma de Madrid (UAM), Spain, 1990] has been doing his doctoral studies on metal preparations and their hydrogenation and the possible existence of nuclear reactions in deuterated metals.

**José Francisco Fernández** (MS, 1988, and PhD, 1994, physics, UAM) has been an advisor professor at UAM since 1992. He is currently conducting research in the Material Physics Department of UAM. His research interests are in the areas of metal hydrides and other topics related to hydrogen as an energy source.

**Carlos Sánchez** (PhD, Universidad Complutense, Madrid, Spain) is a senior professor in the Department of Physics of Materials of UAM. His research interests are in metal hydrides, semiconductor thin films, and conversion and storage of energy.